proceedings

MDPI

Proceedings

Size and Heading of SAR-Detected Ships through the Inertia Tensor †

Luigi Bedini, Marco Righi * and Emanuele Salerno

National Research Council of Italy Institute of Information Science and Technologies, 56124 Pisa, Italy; luigi.bedini@isti.cnr.it (L.B.); emanuele.salerno@isti.cnr.it (E.S.)

* Correspondence: marco.righi@isti.cnr.it

† Presented at the International Workshop on Computational Intelligence for Multimedia Understanding (IWCIM), Kos Island, Greece, 2 September 2017.

Published: 9 January 2018

Abstract: We present a strategy to estimate the heading, the length overall and the beam overall of targets already detected as ships in a wide-swath SAR image acquired by a satellite platform. Such images are often affected by distortions due to marine clutter, spectral leakage, or antenna sidelobes. These can mask the target image, thus hampering the possibility of evaluating the size and the behaviour of the ship. Even in the presence of strong artefacts, we found that the principal inertia axes can help the estimation of the target heading and be included in an iterative procedure to erode the false target features, so to enable a more accurate evaluation of the overall measurements of the ship. Here we introduce our idea and present some results obtained from real SAR images.

Keywords: SAR target classification; ship recognition; inertia tensor

1. Introduction

Image classification is fundamental in many important applications relying on remote-sensed data. Marine surveillance is critical in this sense, for its vital importance in safety and security applications, including safety of life at sea, marine traffic control, and monitoring of smuggling and other illegal activities. High-resolution, satellite-borne synthetic-aperture radar (SAR), is one of the technologies used in marine surveillance, since it provides wide-area images independent of weather and daylight, thus enabling the designated authorities to monitor a large number of targets, provided that fast analysis tools are available. To discover possibly anomalous behaviours in time to take proper countermeasures, an automatic or partially automatic analysis system is essential, able to detect all the ships in the imaged area, to extract their features, and to foresee their possible courses.

In this paper, we assume to have a series of images cropped from a wide-swath SAR image, each containing a single ship, and propose a method to obtain a list of overall sizes and headings estimated from such crops. A number of SAR target classification methods have been proposed in the literature [1–4], based on radiometric and polarimetric features extracted from the image. In actual images, however, this is not always feasible, as polarimetry could not be available and artefacts due to strong reflectors, insufficient sampling rates or antenna sidelobes could be present. The marine clutter, moreover, can affect the data heavily, depending on the sea state, the wind and the ocean currents. In these conditions, provided that the spatial resolution is sufficient, we rely on geometrical features. This is normally difficult for the mentioned distortions but, when accomplished, allows us to estimate the size of a vessel, to make a coarse classification (e.g., small, medium, or large ship), and also to estimate its heading, a first step to evaluate its course and, ultimately, its short-term behaviour.

We propose first to isolate the target by clipping the image outside a mask including the ship and the possible artefacts, then to compute the 2D inertia tensor with respect to the barycentre of the resulting image. The subsequent step is to find the principal inertia axes and to apply a rectangular

mask around the barycentre, so as to include the whole target while cutting out part of the artefacts. Iterating this procedure a few times, a progressively refined estimation of the ship length overall (LOA), beam overall (BOA) and heading is possible. Indeed, when no artefact is cut out anymore, we take the unit vector of the minimum inertia axis as the estimated heading, and the maximum distances between target boundary points along the principal axes as the estimated LOA and BOA. In the absence of further information, such as a detected wake or possible morphological ship features, the heading is estimated up to a 180° ambiguity.

The key to our idea is that, if a figure has a symmetry axis containing the barycentre, this will necessarily coincide with a principal axis of inertia. Now, in our case, we do not look for a general shape, as a ship has always a pseudo-rectangular shape, the main deck being almost symmetric with respect to its fore-and-aft line, which coincides with the axis of minimum inertia. The port-to-starboard line drawn through the barycentre, conversely, is not a symmetry axis, but corresponds to the axis of maximum inertia, orthogonal to the fore-and-aft line and passing, approximately, through the midship section. The size of a rectangular mask enclosing the target but cutting out part of the artefacts can be set up by exploiting a further observation, valid for the ship but not for the artefacts: the distance from the principal axes of any point on the actual ship boundary is never larger than a fixed multiple of its standard deviation. This allows us to adopt a simple criterion based on the standard deviations to size the rectangular mask, thus avoiding general methods [5,6], or methods based on a preliminary detection of the fore-and-aft line in some transform space [7]. The latter are also based on the peculiarities of vessel-type targets, but must rely on a very efficient artefact suppression. Our experimental results demonstrate the effectiveness of this method.

In Section 2, we shortly outline our method, whereas in Section 3 we show some examples of application to real SAR images. Finally, in Section 4, we draw some conclusions and perspectives.

2. Method

Let us denote by F a scalar 2D digital image of a ship target, obtained by clipping a SAR image through a binary mask which is a coarse approximation of the ship shape, possibly distorted by artefacts of various origins. The inertia tensor of this image [8], with respect to the barycentre (x_G, y_G), is

$$I = \begin{bmatrix} I_{xx} & -I_{xy} \\ -I_{xy} & I_{yy} \end{bmatrix} \tag{1}$$

where

$$I_{xx} = \sum_{x,y} F(x,y) \cdot (y - y_G)^2 \tag{2}$$

$$I_{yy} = \sum_{x,y} F(x,y) \cdot (x - x_G)^2 \tag{3}$$

$$I_{xy} = \sum_{x,y} F(x,y) \cdot (x - x_G)(y - y_G) \tag{4}$$

are the inertia moments. An eigenvalue analysis of matrix I yields

$$I = V \cdot \Lambda \cdot V^T \tag{5}$$

where the columns of matrix V, $\mathbf{v}_1 = [v_{11}, v_{21}]^T$ and $\mathbf{v}_2 = [v_{12}, v_{22}]^T$ are the unit vectors of the principal axes of inertia, and the elements of the diagonal matrix Λ, λ_1 and λ_2, are the inertia moments with respect to those axes. The inertia matrix computed with respect to $\mathbf{v}_1$ and $\mathbf{v}_2$ features a vanishing mixed moment $I_{\mathbf{v}_1\mathbf{v}_2}$. If we assume $\lambda_1 < \lambda_2$, the axes parallel to, respectively, $\mathbf{v}_1$ and $\mathbf{v}_2$ passing through the

barycentre are the minimum and maximum inertia axes. For an undistorted ship image, they coincide with the fore-and-aft and the port-to-starboard lines. Their equations are, respectively,

$$y = y_G + m_1 \cdot (x - x_G) \tag{6}$$
$$y = y_G + m_2 \cdot (x - x_G) \tag{7}$$

with $m_1 = v_{21}/v_{11}$ and $m_2 = v_{22}/v_{12}$.

Each point in the image domain has signed distances d_1 and d_2 from the principal axes (6)–(7):

$$d_{1,2}(x,y) = \frac{y - [y_G + m_{1,2}(x - x_G)]}{\sqrt{1 + m_{1,2}^2}} \tag{8}$$

For the points in the image shape, we can compute four quantities, referred to here as *starboard*, *port*, *forward*, and *astern* mean-squared distances from the principal axes. For the 180° heading ambiguity, stern and bow and port and starboard can be interchanged, so the subscripts s, p, f and a used in the following equations are just suggestive.

$$\sigma_s^2 = \frac{1}{N_{1-}} \sum_{(x,y)\in D_{1-}} d_1^2(x,y) \tag{9}$$
$$\sigma_p^2 = \frac{1}{N_{1+}} \sum_{(x,y)\in D_{1+}} d_1^2(x,y) \tag{10}$$
$$\sigma_f^2 = \frac{1}{N_{2-}} \sum_{(x,y)\in D_{2-}} d_2^2(x,y) \tag{11}$$
$$\sigma_a^2 = \frac{1}{N_{2+}} \sum_{(x,y)\in D_{2+}} d_2^2(x,y) \tag{12}$$

where the sets $D_{(1,2)-}$ to $D_{(1,2)+}$ include all the pixels in the target image with d_1 and d_2 assuming, respectively, negative and positive signs, and $N_{(1,2)-}$ to $N_{(1,2)+}$ are their cardinalities. We use the *rms* distances σ_f, σ_a, σ_s and σ_p to build a rectangular mask that includes the whole target and excludes part of the artefacts. When these are removed from the image, refined estimates of the barycentre and the principal axes can be found. Iterating this procedure, we can refine our estimates until nothing falls outside the rectangle.

To establish the size of the mask, we rely again on the pseudo-rectangular shape of a vessel-type target: in our measurements, we found that the distance of the ship boundary from its axes is never larger than 2.07 times the related *rms* distance. Thus, in most cases, a rectangle identified by the *forward line*, at a distance $n_\sigma\sigma_f$ from the maximum-inertia axis, the *aft line*, at a distance $n_\sigma\sigma_a$ from the maximum-inertia axis, the *starboard line*, at a distance $n_\sigma\sigma_s$ from the minimum-inertia axis, and the *port line*, at a distance $n_\sigma\sigma_p$ from the minimum-inertia axis, with $n_\sigma = 2.07$, will enclose the whole ship. This is visualised in the synthetic image of Figure 1, affected by a large artefact that causes a notable displacement of the barycentre and the principal axes.

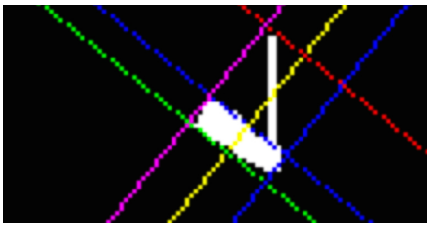

Figure 1. Synthetic target shape affected by a large artefact. An enclosing rectangle is marked by the fore, aft, port and starboard lines, respectively in blue, magenta, red and green.

In this case, the artefact alters so much the *rms* distances that the rectangle encloses completely the detected shape, and the procedure we devised becomes ineffective. We have two ways to check whether such a situation is verified. The first considers the ratio ρ between the area of the target and the area of the enclosing rectangle: in real cases, this ratio is always larger than 0.85 and, in a number of real SAR images we analysed, is seldom less than 0.7. A small ρ thus connotes a target+artefact geometry that is not compatible with the shape of a ship. Also, for an artefact-free shape, it is $\sigma_p \approx \sigma_s$, and σ_f is not significantly different from σ_a. This shortcoming can be remediated, however. If ρ is found to be significantly less than one, the first few (normally, one or two) iterations can be performed by only using the *transverse* and the *longitudinal* root-mean-square distances

$$\sigma_t^2 = \frac{\sigma_s^2 \cdot N_{1-} + \sigma_p^2 \cdot N_{1+}}{N_{1-} + N_{1+}} \tag{13}$$

$$\sigma_l^2 = \frac{\sigma_f^2 \cdot N_{2-} + \sigma_a^2 \cdot N_{2+}}{N_{2-} + N_{2+}} \tag{14}$$

and then centring a rectangle of sides $2n_\sigma\sigma_t$ and $2n_\sigma\sigma_l$ on the barycentre. Part of the artefact now falls outside this rectangle and can be erased. When ρ exceeds a fixed threshold, the iteration can proceed normally.

After a few iterations, the possible residual artefacts do not produce a significant distortion in the estimated axes and enclosing rectangle, so further iterations would leave the image unchanged. An effective stop criterion can thus consider the ratio ρ. When its value remains the same after two consecutive iterations, the algorithm can be stopped. At this point, the minimum-inertia axis approximates the fore-and-aft line of the ship, and can thus be used to estimate its direction. To estimate LOA and BOA, we have two options. The first is to simply put $LOA = n_\sigma(\sigma_f + \sigma_a)$ and $BOA = n_\sigma(\sigma_s + \sigma_p)$. This choice could overestimate the measurements, since n_σ is chosen to safely enclose the whole target but, depending on its particular shape, can leave some room around it. A second option is to compute the distances between the points where the target boundary intersects the principal axes. The presence of false-negative pixels, however, can produce an underestimation of the ship size. Providing both estimates could set useful bounds on LOA and BOA. A further refinement, important for small targets, should be made taking into account the spatial resolution. This is out of the scope of this paper.

Sometimes, we found artifacts that are almost as strong as the target image and with comparable sizes. In these cases, if no privileged symmetry axis is present, the ratio between the estimated LOA and BOA does not fit the values normally found for ships, and the heading estimate is largely uncertain. A ratio between the maximum and the minimum inertia moments that is too close to 1 is an index of either a heavily distorted image or a target that is not classifiable as a ship. In the next section, we show a few concrete examples.

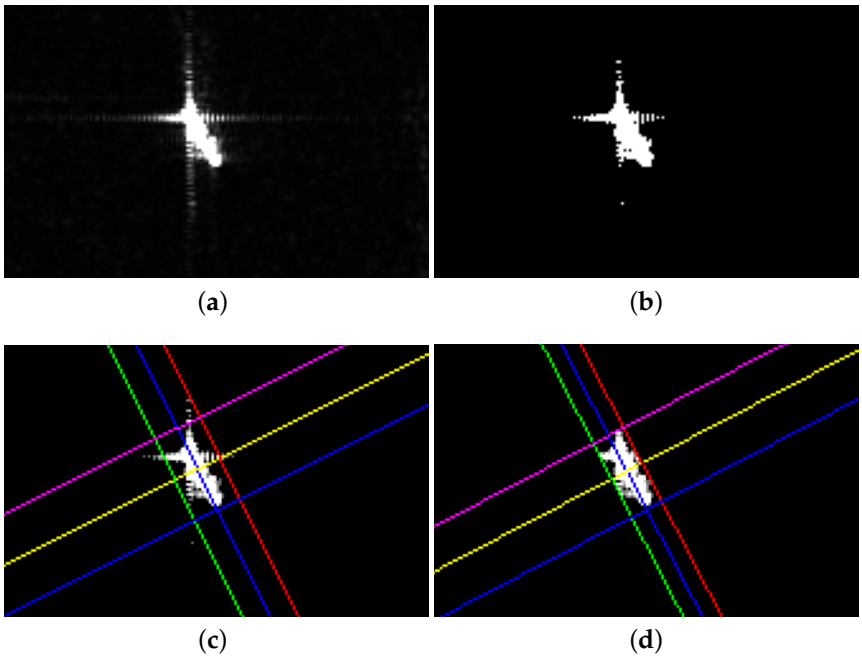

Figure 2. (**a**) Ship target detected in a *Sentinel 1* SAR intensity image, VV polarisation. (**b**) Binary image shape. (**c**) Axes and enclosing rectangle at the first iteration. (**d**) Axes and enclosing rectangle at the fourth iteration.

3. Experiments

The target frames we used to validate the method presented here are cropped from *Sentinel 1* satellite-borne C-band SAR images [9], in both amplitude and intensity, and a fixed pixel size of 10 m $\times$ 10 m. The possible polarisations are VV and VH. No ground truth is available, so our results can only be evaluated on the basis of general *a priori* knowledge. A first example is shown in Figure 2a, an intensity image where the presence of a strong, cross-shaped artefact is apparent. The first step of our procedure consists in building a binary shape where the target pixels are set to 1 and the rest is 0. Being a coarse approximation, this can be done by thresholding, for example, by the classical constant false-alarm rate technique for adaptive thresholding (see, e.g., [10]). The result of a similar procedure is shown in Figure 2b. Figure 2c,d shows how, in the first iteration of our procedure, the artefact falls partly outside the rectangle, and just four iterations are able to isolate accurately the artefact-free shape. Figure 3 shows an example with an amplitude image, clearly more cluttered than the previous one.

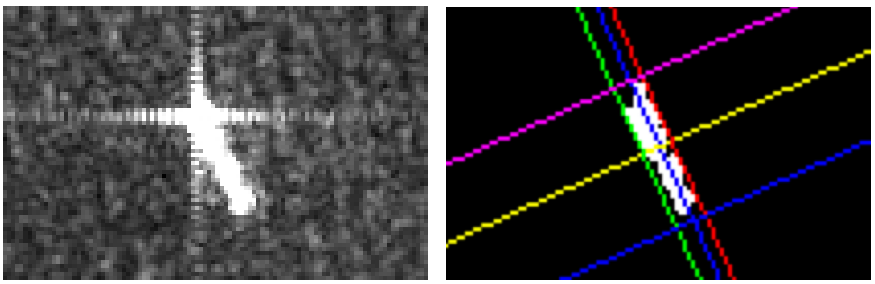

Figure 3. (**a**) Ship target detected in a *Sentinel 1* SAR amplitude image, VV polarisation. (**b**) Axes and enclosing rectangle at the sixth iteration.

A case where the procedure is unsuccessful is shown in Figure 4. Besides having an amplitude comparable with that of the detected target, here the artefact is also of comparable size, thus producing significantly uncertain estimates. In this case, the image is largely saturated and it is difficult to distinguish the target from the artefact, even by visual inspection, as the arms of the cross-shaped artefact are almost aligned with the supposed ship axes. The final value obtained for the area ratio ρ is 0.755, sufficiently large to prevent any automatic system from recognising an anomaly, but the final rectangular mask is almost square, and the principal inertia moments λ_1 and λ_2 are of the same order of magnitude. This is not compatible with common ship shapes, and could be used as an index of failure, as well as a flag to activate some more sophisticated estimation strategy.

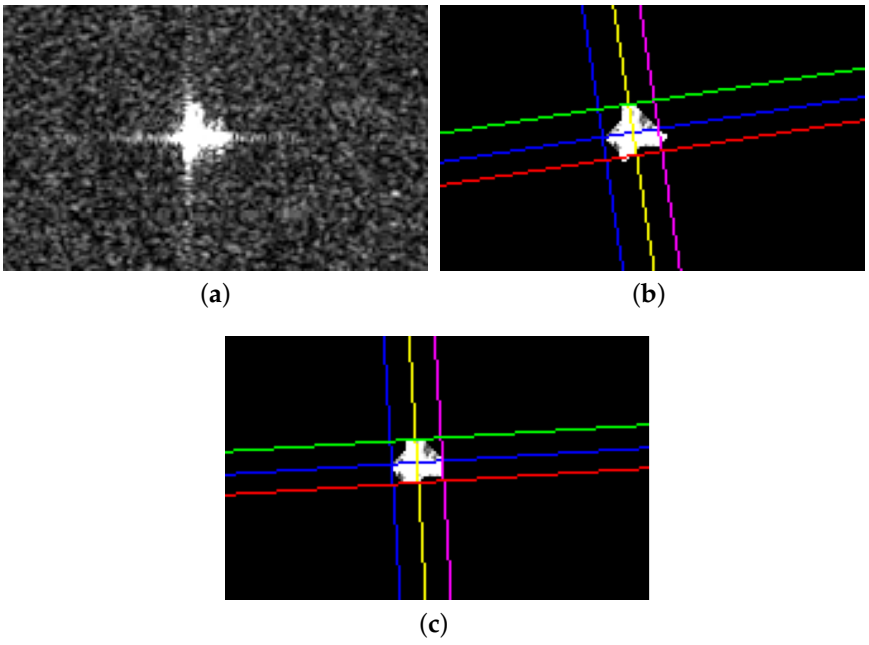

Figure 4. (**a**) Ship target detected in a *Sentinel 1* SAR amplitude image, VH polarisation. (**b**) Size and heading estimates at the first iteration. (**c**) Final size and heading estimates.

4. Conclusions

We present a simple and efficient method to estimate sizes and headings of ships detected in SAR images, where aligning an appropriate rectangular mask to the principal inertia axes avoids some classically expensive processing. With particularly noisy or distorted images, our estimates are not robust. We are studying to establish resolution and signal-to-distortion ratio requirements that are sufficient to guarantee a specified accuracy. We noted that the result often depends significantly on the initial shape assumed, that is, on the thresholding strategy chosen. Without relying on supplemental data or preprocessing, we are now trying to find a method to suitably tune the thresholds. Our next attempt will be to integrate the results from the same target imaged through different transmit-receive polarisations.

This work is intended as a step towards a more complete ship classification method, also based on radiometric and/or polarimetric features, and a more reliable course and speed estimation, possibly based on wake feature extraction and azimuth shift evaluation. Our preliminary studies promise an effective improvement in our classification capabilities.

Acknowledgments: This work has been partially supported by the European Space Agency Technology Project OSIRIS (Optical/SAR data and system Integration for Rush Identification of Ship models).

References

1. Gao, G.; Guo, Y.; Ouyang, K.; Zhou, S. Statistical modeling of pma detector for ship detection in high-resolution dual-polarization sar images. *IEEE Trans. Geosci. Remote Sens.* **2016**, *54*, 4302–4313.
2. Jiang, M.; Yang, X.; Dong, Z.; Fang, S.; Meng, J. Ship classification based on superstructure scattering features in sar images. *IEEE Geosci. Remote Sens. Lett.* **2016**, *13*, 616–620.
3. Lang, H.; Zhang, J.; Zhang, X.; Meng, J. Ship classification in sar image by joint feature and classifier selection. *IEEE Geosci. Remote Sens. Lett.* **2016**, *13*, 212–216.
4. Margarit, G.; Tabasco, A. Ship classification in single-pol sar images based on fuzzy logic. *IEEE Trans. Geosci. Remote Sens.* **2011**, *49*, 3129–3138.
5. Freeman, H.; Shapira, R. Minimum-area encasing rectangle for an arbitrary closed curve. *Commun. ACM* **1975**, *18*, 409–413.
6. Toussaint, G.T. Solving geometric problems with the rotating calipers. In Proceedings of the MELECON '83, Mediterranean Electrotechnical Conference, Athens, Greece, 24–26 May 1983.
7. Tian, X.; Wang, C.; Zhang, H.; Wu, F. Extraction and analysis of structural features of ships in high-resolution sar images. In Proceedings of the 2011 IEEE CIE International Conference on Radar (Radar), Chengdu, China, 24–27 October 2011; pp. 630–633.
8. Landau, L.D.; Lifshitz, E.M. *Mechanics*; Pergamon Press: Oxford, UK, 1969.
9. European Space Agency, Earth Observation Ground Segment Department, SENTINEL-1 SAR Technical Guide, 2016, Available online: https://sentinel.esa.int/web/sentinel/user-guides/sentinel-1-sar (accessed on 13 February 2017).
10. Allard, Y.; Germain, M.; Bonneau, O. Ship detection and characterization using polarimetric sar data. In *Harbour Protection through Data Fusion Technologies*; Shahbazian, E., Ed.; Springer Science + Business Media: New York, NY, USA, 2009; pp. 243–250.